

DESIGN OF AN EFFICIENT MICROWAVE PLASMA REACTOR FOR BULK PRODUCTION OF INORGANIC NANOWIRES

Jeong H. Kim, Vivekanand Kumar, Boris Chernomordik, and Mahendra K. Sunkara*

Department of Chemical Engineering, University of Louisville, Louisville, USA

Key words: plasma, atmospheric pressure, microwave, argon, oxygen, nanowire, nanoparticle, metal oxide

Abstract: We report the design of an atmospheric microwave plasma reactor to produce metal oxide nanowires. The reactor has a custom-made tapered waveguide and a 2.45GHz, 3kW (MKS ASTeX) magnetron and power supply unit for generating highly dense microwave plasma. As a result, a high temperature microwave plasma flame inside a quartz tube of 2 in. diameter and 1 ft. length was generated to produce metal oxide nanowires and nanoparticles. High Frequency Structure Simulator (HFSS) software was used to simulate the electric field distribution inside the dielectric tube.

Mikrovalovni plazemski reaktor za učinkovito izdelavo velike količine anorganskih nanožičk

Ključne besede: plazma, atmosferski tlak, mikrovalovi, argon, kisik, nanožičke, nanodelci, kovinski oksidor

Izveček: Predstavljamo konstrukcijske rešitve pri razvoju in izdelavi plazemskega reaktorja za proizvodnjo nanožičk kovinskih oksidov. Reaktor značilno deluje pri atmosferskem tlaku. Z razvojem novega posebej prilagojenega valovnega vodnika, magnetrona z največjo močjo 3kW in frekvenco 2.45 GHz in ustreznega močnostnega napajalnika smo uspeli v razelektrivni komori dobiti izredno gosto mikrovalovno plazmo. Znotraj kvarčne cevi s premerom okoli 5 cm in dolžino okoli 0.5 m ustvarimo plamen izredno vroče plazme, v katerem poteka sinteza nanožičk in drugih nanodelcev kovinskih oksidov. Porazdelitev električnega polja smo tudi izračunali z uporabo primerne programske opreme.

1 Introduction

Plasma has been used for various interesting applications particularly with production of nanomaterials /1-5/, quantum dots /6-8/, carbon nanostructures /9-12/, surface treatment /13-18/, decomposition /19-21/, and functional treatment /22-26/. One popular process for producing metal oxide nanowires is plasma-enhanced chemical vapor deposition (PECVD) /27/. Inorganic nanowires are an interesting set of nanostructures with a lot of potential applications in the fields such as solar cells /28/, Li-ion batteries /29/, nano-composites /30-32/, gas sensing /33-35/, and others. In many of these applications, nanowires are needed in large quantities. Thus, an efficient method for bulk production of nanowires is needed. The methods employed so far include catalyst-based Vapor Liquid Solid (VLS) /36/, thermal evaporation /37/, laser ablation /38/, hydrothermal synthesis /39/, sol-gel /40/, electrodeposition, plasma foil oxidation /41-44/ and others. None of these methods, however, are capable of producing nanowires in bulk amounts because they are all based on the use of a substrate or template which limits the amount of material that can be synthesized /45/. A truly bulk production system would require a vertical reactor with the ability to treat the metal powders continuously in gas phase and sweep the reacted species away from the reaction zone.

Design of such a reactor would invariably involve plasma or a combustion flame. The system would also require a fast, high through-put system, direct reaction (without the need of any substrate), highly dense dissociated reactive

gases, large volume, and a stable and efficient flame system. An atmospheric system /46-48/ would be less expensive than vacuum, and would likewise be easier and faster to operate. The combustion flame method has been used to produce nanoparticles by completely vaporizing the metal powder /49/. However, it is prone to carbon contamination with the vapor sources-(e.g from oxygen-acetylene (or C_nH_m))-and is not ideal for creating molten metal conditions required for nanowires. The plasma employed in such a reactor could be based on medium frequency (MF), radio frequency (RF), capacitively/inductively coupled plasma (C/ICP), microwave (MW), and direct current (DC) /50-53/. MF, RF, and C/ICP require the use of a co-axial cable, which makes it difficult to produce plasma for bulk production because the cable would melt if high density plasma is obtained.

DC plasma uses electrodes which degrade easily under atmospheric conditions because of presence of oxygen in the gas species. This requires frequent change of electrodes which causes contamination problems /54-55/. To avoid this problem, an electrode-less high temperature plasma can be used to produce metal oxide nanowires under atmospheric pressure. RF uses co-axial cables to generate plasma, which makes it difficult to make large volume, high temperature plasma under atmospheric conditions with low power (1 to 3 kW). RF can also be used at atmospheric conditions for producing nanowires but at higher powers, e.g 30kW /56/.

Microwave energy can be used to generate large volume plasma without electrodes, thus avoiding contamination

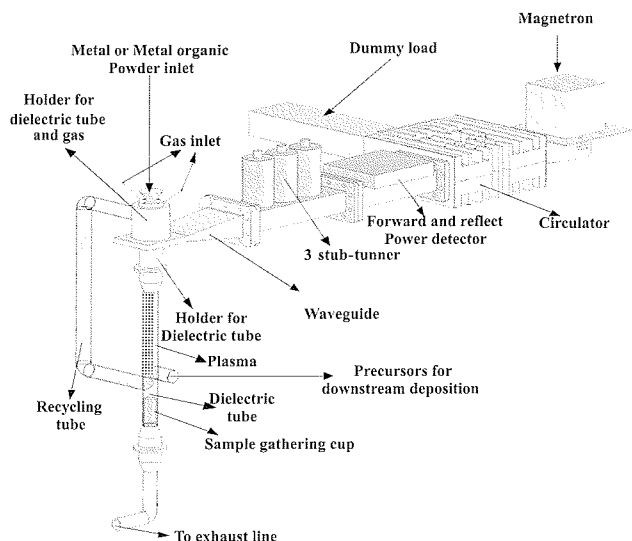


Fig. 1: A simplified schematic of the microwave plasma reactor.

/57/. The low electrical resistance loss, no need of any dielectric substance, low radiation loss, and ability to transfer high power to generate high density atmospheric microwave plasma makes it an ideal solution for high-throughput continuous metal-oxide nanowire synthesis. Therefore, we used a microwave source to produce plasma in this reactor.

2 Experimental and reactor set up

A reactor was designed that could efficiently generate highly dense microwave plasma discharges in a jet like manner confined inside tubes operating at pressures ranging from few Torr to atm. and at powers ranging from 300 W - 3 kW. A simplified schematic of the reactor set-up is shown in Figure 1. The set-up includes a plasma producing source (consisting of magnetron, forward and reflect power detector, dummy load, 3 stub-tuner and a circulator); a custom made waveguide; an entry port for feed source; an entry port for gases; a holder for gases and metal powder inlet; a dielectric tube such as quartz; a sample gathering cup; and an exit port for exhaust gases. The electric field (at 2.45 GHz microwave frequency) produced by magnetron and transported through the rectangular WR284 channels is concentrated in the middle of the dielectric tube in the waveguide which is appropriately designed (discussed later). A microwave plasma head with 3kW MKS Inst. AS-TeX power supply and a 2.45GHz magnetron is used. A metallic rod with pointed end is used to ignite the plasma after introducing Ar gas (2 standard liter per minute (slpm)) and is immediately removed. Subsequently the reacting gases (air 8-14 slpm, O₂ 500 sccm) are introduced and plasma is stabilized by stub-tuner and the reflected power is tuned to zero. The plasma jet length is about 12-15 in. as shown in the Figure 2. The quartz tube diameter is 1 to 1.5 in. and the length is 3 ft.

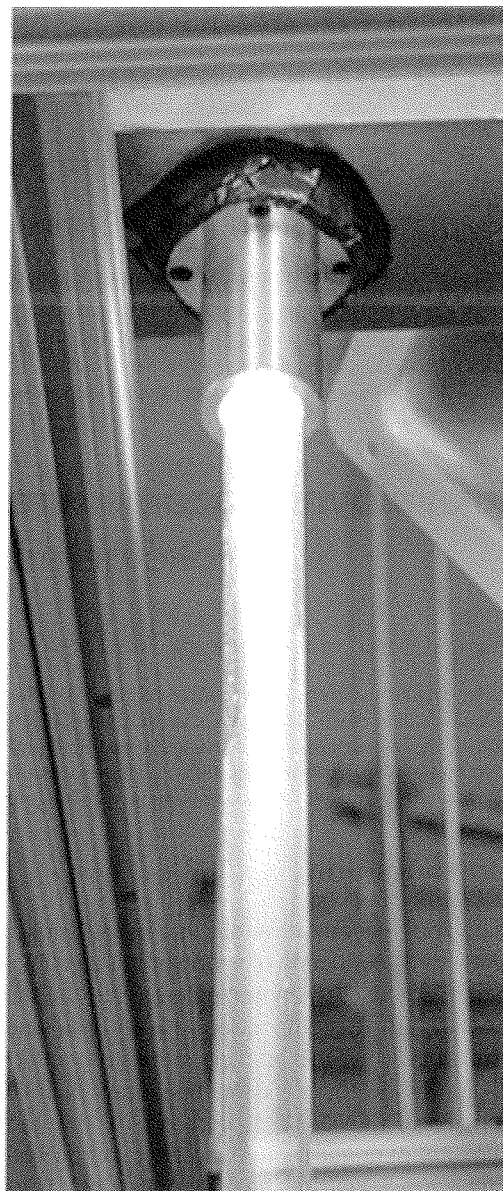


Fig. 2: Photograph of the microwave plasma discharge at 2 kW power.

Various gases are mixed in a single gas line and fed at the top of the reactor at the two diametrically opposite ends of the gas port holder in the gas delivery. Figure 3 shows the schematic of the port for gas delivery system. The gas is delivered tangentially at an angle of 60° with the vertical. The angle of the gas inlet produces a helical gas path around the periphery of the dielectric tube with downward momentum when sheath gas is delivered through the gas inlet. By delivering sheath gas (air, 8-14 slpm) via this system, the high density plasma discharge is confined near the center of the tube. Thus, contact of the plasma with the dielectric tube is avoided and the peripherally-confined sheath gas prevents the transmission of heat from the plasma to the dielectric tube. This helps to contain the plasma and to keep the dielectric tube cool during the operation of the reactor for any desired period of time. Air, oxygen, and nitrogen etc. could be used as sheath gases. The die-

lectric tube is important so that the plasma distributes uniformly within the tube. Preferably, the plasma should occupy a large portion of the tube cross section without touching or melting the tube. The desired metal powder (or metal-containing precursor) is delivered into the dielectric tube via gravity feed and is conveyed through the plasma by gravity. The collector is a cup which is attached at the bottom of tube while leaving space for exhaust gases to escape through. The exhaust line is connected to a mechanical pump which also sustains the plasma discharge by maintaining the optimum amount of gases in the reactor. The batch plasma reactor can be converted in to a continuous reactor by recycling partially converted products through recycling tube and combining with incoming feeds as discussed later.

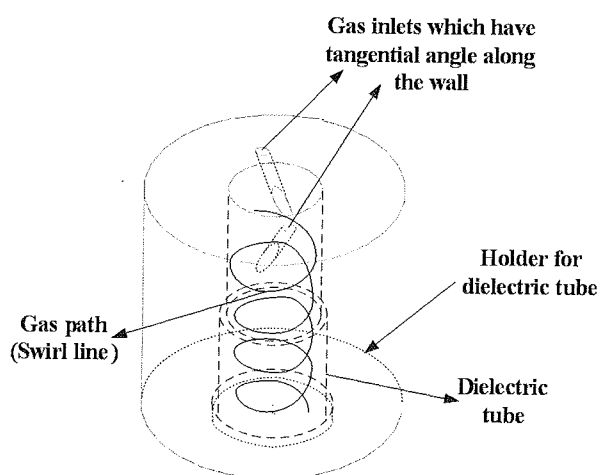


Fig. 3: Schematic showing the gas delivery system at a specified angle.

3 Processing scheme and results

The metal oxide nanowires of tin and zinc were produced using the above mentioned microwave plasma reactor operating at 1000-2000 W and 2.45 GHz in an atmosphere of 8-15 slpm air as sheath gas, and a plasma forming gas of 2-4 slpm argon and 100-700 sccm of oxygen (used as oxidative gas) at atmospheric pressure. In this process, the metal powder is supplied from the top into the microwave plasma jet and the nanowires are collected at the bottom of the tube. Gases and metals react at the center of the quartz tube near the plasma flame head and continue reacting as they fall under gravity along the plasma flame length. The length of the plasma can be varied by changing the gas flow rates or by changing the microwave power. The gas flow rate can be controlled by the mass flow controllers (MFC) and also by the mechanical pump. The products are collected at the bottom of the reactor. Figure 4a and b shows the Scanning Electron Micrographs (Nova Nano-600 Scanning Electron Microscope) of these as-synthesized metal oxide nanowires. From the SEM images we find that all these nanowires are typically 1-10 μm in length and less than 100 nm in diameter. At higher applied

powers nanoparticles of alumina were produced using micron-sized Aluminum metal shown in Figure 4c. These nanoparticles are less than 100 nm in size and are uniform in size distribution.

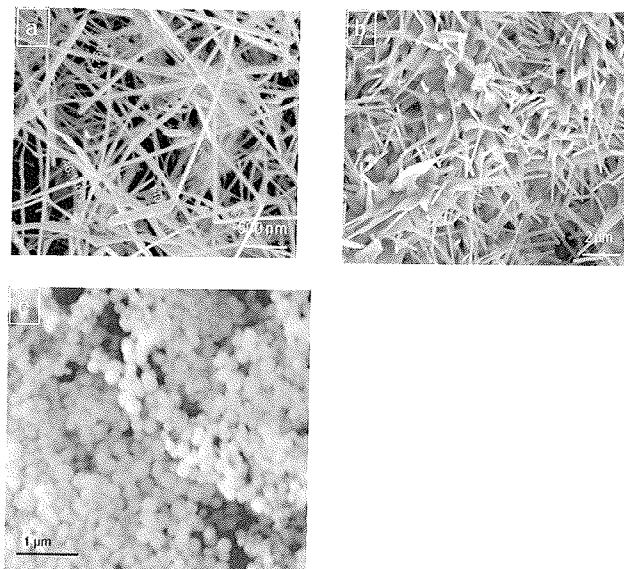


Fig. 4: As-synthesized nanowires of (a) tin oxide, (b) zinc oxide, (c) and nanoparticles of alumina.

3.1 Reactor Simulation and Analysis

The design of the waveguide to concentrate the electric field is a critical factor in this reactor. A perfectly designed waveguide would concentrate the maximum intensity of the electric field at a point where the dielectric break-down of the gases can occur by introducing plasma forming gases to strike the plasma. The design was done by simulating the electric field patterns inside the waveguide. Theoretically, the strongest electric field position is $\lambda/4$. The magnetic field can be ignored in the TE₁₀ mode because of lower magnitude compared to the electric field.

For a 2.45 GHz microwave ($\lambda=12.24\text{cm}$) using WR284 waveguide, where $a = 72.14 \text{ mm} = 2.84 \text{ in}$ (a is width of the larger side of rectangular channel), the cut off wavelength $\lambda_c = 2a = 14.43 \text{ cm}$, the cut off frequency $f_c = c/\lambda_c = 1.6 \text{ GHz}$, λ_g the waveguide wavelength can be calculated using equation (1) /24/:

$$\lambda_g = \frac{\lambda}{\sqrt{1 - \left(\frac{f_c}{f}\right)^2}} = \frac{12.24\text{cm}}{\sqrt{1 - \left(\frac{1.6}{2.45}\right)^2}} = 21.34\text{cm} \quad (1)$$

Electric field intensity simulations were performed for two different waveguide shapes - rectangular and tapered - in a WR284 wave guide as shown in Figure 5. The tapered waveguide was preferred over rectangular one because the maximum electric field intensity is more than doubled (170,000 vs. 80,000 V/m in the two cases). The tapered shape also causes the gradual change in the impedance at the end of waveguide and thus there is no formation of

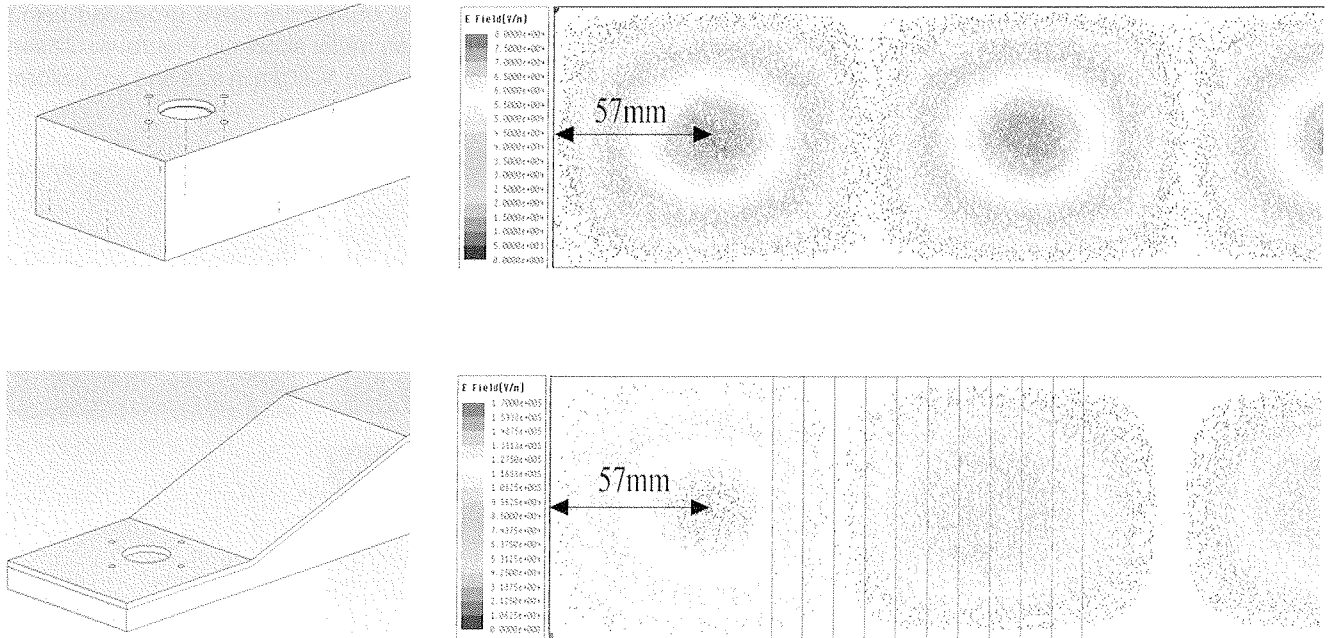


Fig. 5: Rectangular and tapered waveguides and the electric field intensities using them. The top image shows the rectangular and bottom shows the tapered waveguide.

“standing waves” (as in a rectangular waveguide) and hence has higher efficiency. Note that the theoretical $\lambda_g/4$ in a WR284 waveguide is $\lambda_g/4 = 53.36$ mm whereas the simulated $\lambda_g/4 = 57$ mm, as shown in Fig. 5, slightly differs.

The simulation result for electric field intensities at the shortened end of the tapered waveguide using quartz and ceramic tubes with varying diameters and thickness are shown in Table 1. $\lambda_g/4$, where the electric field is strongest is 53.35mm without a dielectric tube from equation 1. The

simulated distance for maximum electric field intensity in a tapered and rectangular waveguide without any tube is 57 mm which differs only slightly from the theoretical value. As shown in Table 1, the maximum field intensity distance ($\lambda_g/4$) increases with larger tube diameters for same thickness of tube and decreases with larger tube thicknesses for the same diameter. Also for the same diameter and thickness the $\lambda_g/4$ distance is lower in the case of a material with higher dielectric constant (e.g. compare the values for 1 in. and 1 mm thick quartz and ceramic tubes).The

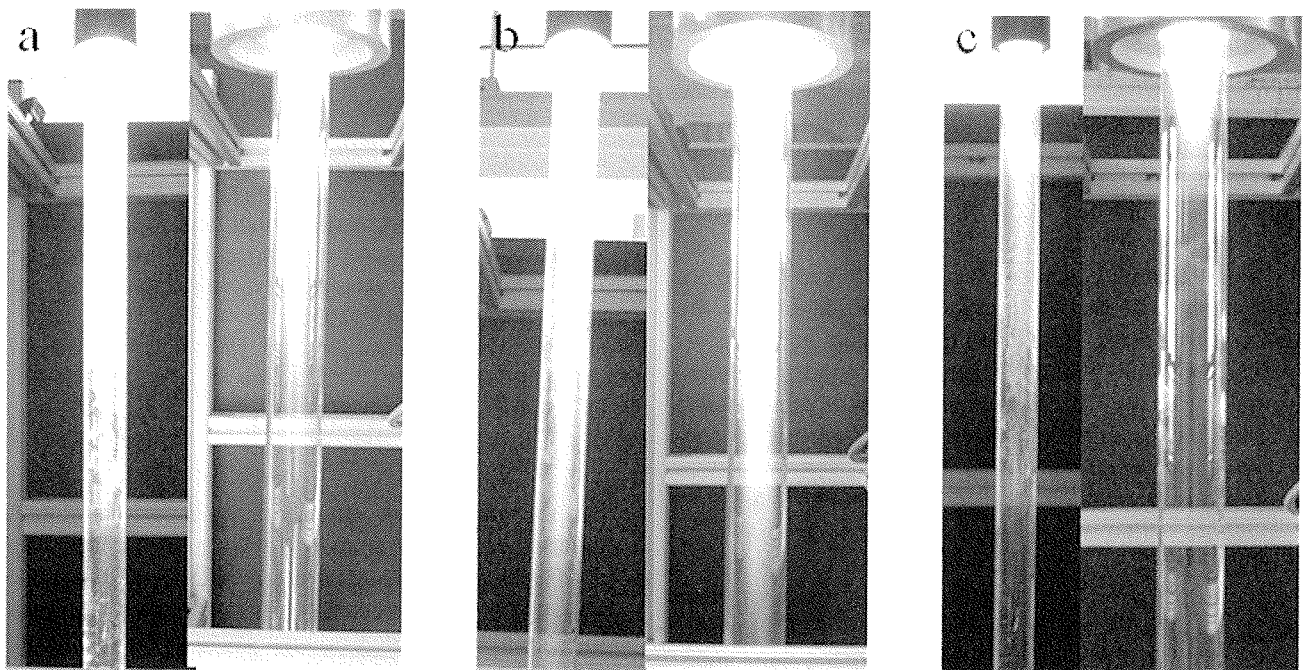


Fig. 6: Plasma discharge inside quartz tube diameters of 1 in (left) and 1.5 in. (right) using (a) air, (b) oxygen, and (c) nitrogen. The applied power and gas flow rate are 1.2 kW and 12 slpm respectively.

effect can possibly be due to the dielectric effect, which acts as the shield of the electrical energy. So, the electric field line is changed with dielectric tube material (dielectric constants for ceramic, quartz and air are 10, 4.2 and 1 respectively) and thickness. Materials with higher dielectric constants and likewise thicker materials show pronounced shielding effects. The waveguide was designed in such a way so that the maximum electric field lines are located at the middle of holes created for the insertion of vertical quartz tube. The tube would melt due to arcing if the maximum electric field lines are at the periphery of the tube. Thus, the design of waveguide would depend on the diameter and thickness of the dielectric material being used. This principle was used in the design of a waveguide to generate stable and strong plasma flame.

3.2 Other design issues

The design of the microwave plasma reactor involves many issues such as: design of metal powder and gas delivery system, design of waveguide, choice of quartz tube diameter and the reacting gases, plasma flame stabilization, minimization of product deposition on the quartz tube wall, design of bottom product collection system, and product efficiency. Design of wave guide and metal powder and gas delivery system has been explained earlier. An appropriately chosen quartz tube diameter serves many purposes. It avoids the contact of hot plasma flame with the wall of the quartz tube and hence avoids the tube melting. The sheath gas is also important for the purpose of carrying out the reaction.

Table 1: Electric field simulation results for $\lambda g/4$ distances in different materials of different thickness and diameters

Wave guide type used	Theoretical calculation	Rectangular waveguide	Tapered waveguide
Distance mm	53.35	57	57
1 in. quartz tube - tapered waveguide			
Thickness	1mm	3mm	5mm
Distance mm	60.96	55.88	50.8
1.5 in. quartz tube - tapered waveguide			
Thickness	1mm	3mm	5mm
Distance mm	66.55	61.09	58.42
1 in. ceramic tube - tapered waveguide			
Thickness	1mm	3mm	5mm
Distance mm	53.34	31.75	29.08

Figure 6 shows the plasma discharges in two different diameter of quartz tube (1 in and 1.5 in) using air (Figure 6a), oxygen (Figure 6b), and nitrogen (Figure 6c) at 1.2 kW plasma power and 12 slpm gas flow. The flame in 1 in. quartz tube is shown in the left while that in the 1.5 in. is shown in the right of each figure. As evident from Figure 6, a 1 in. tube diameter results in significant closeness of plas-

ma flame with the tube thereby melting the tube with prolonged exposure. The plasma flame is brightest and most reactive using oxygen, diminishes in the air, and is least reactive in nitrogen flame as shown in Figure 6c. The nitrogen plasma flame turns from violet to yellow to white with the increase in applied powder. Hence we chose 1.5 in. tube diameter and air or oxygen as the sheath gas. The choice of sheath gas also depends on the required product. For example, to produce sulfide and nitride compounds, N and S containing gases (e.g. NH_3 and H_2S) need to be introduced in an oxygen free environment. The plasma flame has tendency to overflow at the top of the reactor thereby creating difficulty in pouring the metal powders from the top. The flame can be directed downwards by using a mechanical pump which quickly evacuates feed gases. A significant portion of the product formed goes to waste by depositing on the walls of the quartz tube if the tube diameter is small. Although 1.5 in. quartz tube is barely sufficient for treatment of large amount of metal powders, a 4 in. or higher diameter quartz tube would be appropriate to avoid deposition of products onto the wall. However, striking and maintaining the plasma in a 4 in. diameter tube poses significant challenge and hence we used 1.5 in. tube diameter. Figure 7 shows the schematic and photograph of a product collection system consisting of a quartz cup placed inside a 4 way 4"-2" reducing cross. The gravity falling product impacts the bottom of the cup and also other finer products are entrained by the gas and can be captured by placing a filter paper in the side-way exit for the exhaust out-let.

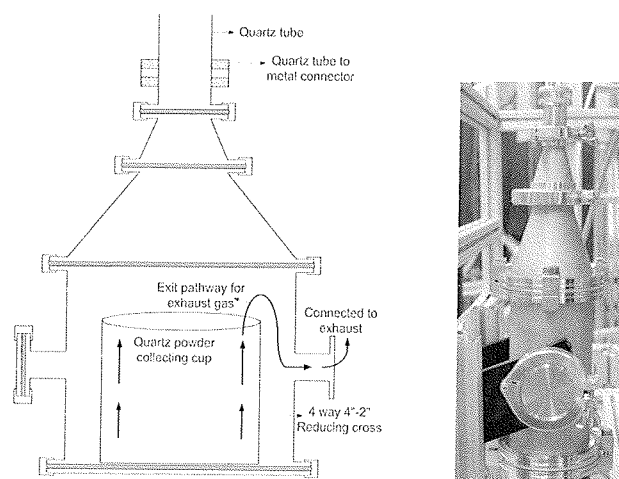


Fig. 7: (a) Schematic and (b) photograph of product collection cup used in the reactor.

The height of the cup should be higher than the height of the side-way exit and also its cross-sectional area should occupy a large portion of the bottom of reducing cross on which it rests. The product efficiency (i.e. % of required nanowires or nanoparticles vs. unreacted or agglomerated materials) can be improved by recycling the product as shown in Figure 8. The recycling system makes use of a cyclone separator and an entraining gas (carrying the un-

reacted and heavier products) forming part of the gases introduced at the top of the reactor. The final product is the outcome of cyclone separation. The recycling system, which makes for a continuous way of producing nanowires, is limited by two parameters: (1) the maximum solid loading in the entraining gas and also (2) the maximum solid which can be treated by the plasma flame. So at steady state these two should be equal and they together with the efficiency with which heavier and finer particles get separated will determine the production rate. Recycling a part of the product not only improves the efficiency but also leads to a continuous production of products.

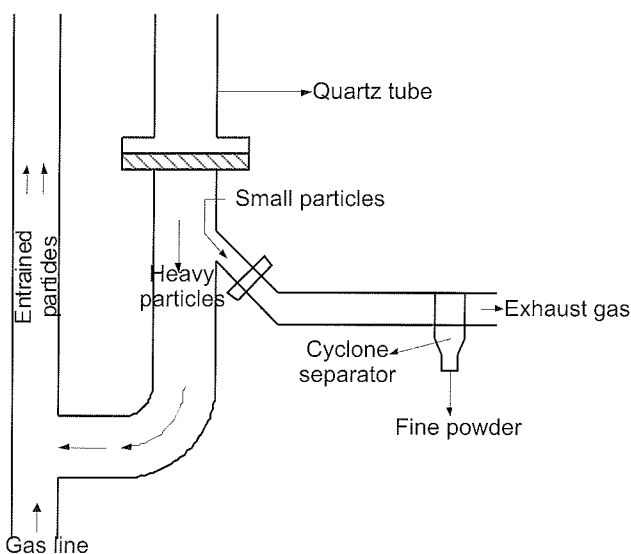


Fig. 8: Schematic of the recycling system.

4 Conclusions

A new microwave plasma reactor was successfully designed to produce highly dense plasma. The waveguide design is the key aspect of this reactor. The design involves several key issues such as gas and metal powder delivery, plasma flame stabilization, product collection cup. Using this reactor metal oxide nanowires and nanoparticles were produced in bulk (kg) quantities.

Acknowledgements

Authors gratefully acknowledge support from US Army Space Missile Defense Command (W9113M-04-C-0024), US Department of Energy (DE-FG02-05ER64071 and DE-FG02-05ER64071) and the U.S. Department of Energy/Kentucky Rural Energy Consortium (DE-FG36-05G085013A).

References

/1/ K. Ostrikov and A. B. Murphy, *J. Phys. D: Appl. Phys.*, vol. 40, pp. 2223-2241, 2007.

/2/ S. Sharma and M. K. Sunkara, *Nanotechnology*, vol. 15, pp. 130-134, 2004.

/3/ K. Ostrikov, *Rev. Mod. Phys.*, vol. 77, no.2, pp. 489-511, 2005.

/4/ E. Tam, I. Levchenko and K. Ostrikov, *J. Phys. D: Appl. Phys.*, vol. 100, no.3, art. no. 036104, 2006.

/5/ U. Cvelbar, K. Ostrikov and M. Mozetic, *Nanotechnology*, vol. 19, no. 40, art. no. 405605, 2008.

/6/ J. C. Ho, I. Levchenko, and K. Ostrikov, *J. Appl. Phys.*, vol. 101, art. no. 094309, 2007.

/7/ Q.J. Cheng, S. Xu, J.D. Long et al., *Appl. Phys. Lett.*, vol. 90, no. 17, art. no. 173112, 2007.

/8/ I. Levchenko, A.E. Rider, and K. Ostrikov, *Appl. Phys. Lett.*, vol. 90, no. 19, art. no. 193110, 2007.

/9/ K. Ostrikov, Z.L.Tlakatze, P. P. Rutkevych, J. D. Long, S. Xu, I. Denysenko, *Cont. to Plasma Phys.*, vol. 45, pp. 514-521, 2005.

/10/ I. B. Denysenko, S. Xu, J. D. Long, P. P. Rutkevych, N. A. Azarenkov, and K. Ostrikov, *J. Appl. Phys.*, vol. 95, pp. 2713-2724, 2004.

/11/ I. Levchenko et al., *J. Phys. D : Appl. Phys.*, vol. 41, no. 13, art. no. 132004, 2008.

/12/ I. Denysenko et al., *J. Appl. Phys.*, vol. 104, no. 7, art. no. 073301, 2008.

/13/ U. Cvelbar, S. Pejovnik, M. Mozetic, and A. Zalar, *Appl. Surf. Sc.*, vol. 210, pp. 255-261, 2003.

/14/ J.-H. Kim, G. Liu, and S. H. Kim, *J. Mater. Chem.*, vol. 16, pp. 977-981, 2006.

/15/ C. Canal, F. Gaboriau, S. Villeger et al., *Int. J. Pharm.*, vol. 367, no. 1-2, pp. 155-161, 2009.

/16/ C. Canal, F. Gaboriau, A. Ricard et al., *Plasma Chem. Plasma Proces.*, vol. 27, no.4, pp. 404-413, 2007.

/17/ A. Ricard et al., *Plasma Chem. Plasma Proces.*, vol. 5, no.9, pp. 867-873, 2008.

/18/ C. Canal, R. Molina, P. Erra, and A. Ricard, *Eur. Phys. J. Appl. Phys.*, vol. 36, no. 35-36, 2006.

/19/ J. H. Hsieh and C. Li, *Thin Solid Films*, vol. 504, pp. 101-103, 2006.

/20/ M. Mafra et al., *Key Eng. Mater.*, vol. 373-374, pp. 421-425, 2008.

/21/ N. Krstulović, I. Labazan, S. Milošević et al, *J. Phys. D : Appl. Phys.*, vol. 39, pp. 3799-3804, 2006.

/22/ T. Vrlinic et al., *Surf. Interface Anal.*, vol. 39, no. 6, pp. 467-481, 2007.

/23/ U. Cvelbar et al., *Appl. Surf. Sci.*, vol. 253, no. 21, pp. 8669-8673, 2007.

/24/ C. Canal, S. Villeger, S. Cousty, B. Rouffet, J.P. Sarrette, P. Erra, A. Ricard, *Appl. Surf. Sci.*, vol. 254, no. 18, pp. 5959-5966, 2008.

/25/ U. Cvelbar Sci., B. Markoli, I. Poberaj, A. Zalar, L. Kosec, and S. Spaic, *Appl. Surf. Sci.*, vol. 253, pp. 1861-1865, 2006.

/26/ A. Vesel et al., *Surf. Interface Anal.*, vol. 40, no.11, pp. 1444-1453, 2008.

/27/ D. Mariotti, H. Lindstrom, A.C. Bose, *Nanotechnology*, vol. 19, no. 49, 495302, 2008.

/28/ S. Gubbala, V. Chakrapani, V. Kumar, and M. K. Sunkara, *Adv. Func. Mater.*, vol. 18, pp. 2411-2418, 2008.

/29/ P. Meduri, C. Pendyala, V. Kumar, G. U. Sumanasekera, and M. K. Sunkara, *Nano Lett.*, vol. 9, pp. 612-616, 2009.

/30/ S. R. C. Vivekchand, K. C. Kam, G. Gundiah, A. Govindaraj, A. K. Cheetham, and C. N. R. Rao, *J. Mater. Chem.*, vol. 15, pp. 4922-4927, 2005.

/31/ U. Cvelbar, M. Mozetic, and M.Klanjsek Gunde, *IEEE Trans. Plasm. Sci.*, vol. 33, no.2, pp. 236-237, 2005.

/32/ M. Klanjsek Gunde, M. Kunaver et al., *Prog. Ora. Coat*, vol. 54, no. 2, pp. 12-16, 2006

- /33/ B. Deb, S. Desai, G. U. Sumanasekera, and M. K. Sunkara, *Nanotechnology*, pp. 285501-285507, 2007.
- /34/ U. Cvelbar, K. Ostrikov, A. Drenik, and M. Mozetic, *Appl. Phys. Lett.*, vol. 93, no. 13, art. no. 133505, 2008.
- /35/ A. Drenik, U. Cvelbar, K. Ostrikov, and M. Mozetic, *J. Appl. Phys. D : Appl. Phys.*, vol. 41, no. 11, art. no. 115201, 2008.
- /36/ R. S. Wagner and W. C. Ellis, *Appl. Phys. Lett.*, vol. 4, pp. 89-90, 1964.
- /37/ B. D. Yao, Y. F. Chan, and N. Wang, *Appl. Phys. Lett.*, vol. 81, pp. 757-759, 2002.
- /38/ A. M. Morales and C. M. Lieber, *Science*, vol. 279, pp. 208-211, 1998.
- /39/ Z. Li, X. Huang, J. Liu, and H. Ai, *Mater. Lett.*, vol. 62, pp. 2507-2511, 2008.
- /40/ M. Zhang, Y. Bando, and K. Wada, *J. Mater. Sc. Lett.*, vol. 20, pp. 167-170, 2001.
- /41/ M. Mozetic, U. Cvelbar, M. K. Sunkara, and S. Vaddiraju, *Adv. Mater.*, vol. 17, pp. 2138-2142, 2005.
- /42/ U. Cvelbar et al., *Small*, vol. 4, no.4, pp. 1610-1614, 2008.
- /43/ Z.Q. Chen et al., *Chem. Mater.*, vol. 20, no.9, pp. 3224-3228, 2008.
- /44/ U. Cvelbar and K. Ostrikov, *Cryst. Growth Des.*, vol.8, no.12, pp. 4347-4349, 2008.
- /45/ V. Kumar, J. H. Kim, C. Pendyala, B. Chernomordik, and M. K. Sunkara, *J. Phys. Chem. C*, vol. 112, pp. 17750-17754, 2008.
- /46/ V. Hody et al., *Plasma Chem. Plasma Process*, vol. 26, no. 3, pp. 251-266, 2006.
- /47/ G. Arnoult, R.P. Cardoso, T. Belmonte and G. Henrion, *Appl. Phys. Lett.*, vol. 93, no. 19, art. no. 191507, 2008.
- /48/ T. Belmonte, R.P. Cardoso, G. Henrion, and F. Kosior, *J. Phys. D: Appl. Phys.*, vol. 40, no. 23, pp. 7343-7356, 2007.
- /49/ J. B. Donnet, H. Oulanti, T. L. Huu, and M. Schmitt, *Carbon*, vol. 44, pp. 374-380, 2006.
- /50/ M. Mozetic, A. Vesel, U. Cvelbar et al., *Plasma Chem. Plasma Process.*, vol. 26, no.2, pp. 236-237.
- /51/ M. Mozetic, U. Cvelbar, A. Vesel, et al., *J. Appl. Phys.*, vol. 97, no. 10, art. no. 103308, 2005.
- /52/ K.N. Ostrikov, S. Xu, M.Y. Yu, *J. Appl. Phys.*, vol. 88, no. 5, pp. 2268-2271, 2000.
- /53/ A. Ricard, F. Gaboriau, and C. Canal, *Surf. Coat. Tech.*, vol. 202, pp. 5220-5224, 2008.
- /54/ S.V. Vladimirov et al., *Phys. Rev. E*, vol. 58, no. 6, pp. 8046-8048, 1998.
- /55/ K.N. Ostrikov, M.Y. Yu and H. Sugai, *J. Appl. Phys.*, vol. 86, no.5, pp. 2425-2430, 1999.
- /56/ H. Peng, Y. Fangli, B. Liuyang, L. Jinlin, and C. Yunfa, *J. Phys. Chem. C*, vol. 111, pp. 194-200, 2007.
- /57/ R.P. Cardoso, T. Belmonte, P. Keravec, F. Kosior and G. Henrion, *J. Phys.D: Appl. Phys.*, vol. 40, no.5, pp. 1394-1400, 2007.

*Jeong H. Kim, Vivekanand Kumar, Boris Chernomordik, and Mahendra K. Sunkara**
Department of Chemical Engineering, University of Louisville, Louisville, KY 40292
Corresponding Author: mahendra@louisville.edu

Prispelo (Arrived): 17.09.2008 Sprejeto (Accepted): 15.12.2008